Electronic Supplementary Material (ESI) for Environmental Science: Water Research & Technology.
This journal is © The Royal Society of Chemistry 2024

Simultaneous mitigation of multiple pollution in urban stormwater systems illicitly connected with sewage systems by Fe(VI)-based process

Jinglong Hu [a, b], Ruihua Zhang [a, b], Zhengdi Wu [a, b], Cheng Ye [a, b], Wenyuan Yang [a, b], Wenhai Chu [a, b, *]

[a] State Key Laboratory of Pollution Control and Resources Reuse, College of Environmental Science and Engineering, Tongji University, Shanghai, 200092, China

[b] Ministry of Education Key Laboratory of Yangtze River Water Environment, Tongji University, Shanghai 200092, China

*Corresponding author:

Tel.: +8618721871983; fax: +86 21 65986839

E-mail address: feedwater@126.com; 1world1water@tongji.edu.cn

Address: Room 407, National Engineering Research Center for Urban Pollution Control, Tongji University,

1239 Siping Road, Yangpu District, Shanghai 200092, China

Text S1. Chemicals and reagents. (Page S3)
Text S2. The measurement of fluorescence excitation-emission matrix (EEM). (Page S4)
Text S3. The measurement of size-exclusion chromatography-organic carbon detector (SEC-OCD). (Page S5)
Text S4. UPLC conditions for emerging contaminants analysis. (Page S6)
Text S5. Quantification Method of Fe(VI). (Page S7)
Table S1. Major quality parameters for sewage. (Page S8)
Table S2. Analytical methods and conditions for DBPs measurement. (Page S9)
Table S3. Characteristics, sources and limit of quantitation of the DBPs. (Page S10)
Fig S1. Fit of PCT oxidation by Fe(VI) with second-order reaction kinetics at different molar ratios of organics to Fe(VI). Experimental conditions: $[Fe(VI)]_0 = 200$ μM. (Page S11)
Fig S2. The actual removal of PCT (a, b) and IBP (c, d) by Fe(VI) and Fe(VI) /Fe(III) processes. (Page S12)
Fig S3. Effect of Fe(VI) dosage on DBP formation in sewage under Fe(VI)-based process. (Page S13)
Fig S4. Effect of Fe(III) and Fe(VI) dosage on DBP formation in sewage under Fe(VI)/ Fe(III)-based process. (Page S14)
Fig S5. Effect of Fe(III) and Fe(VI) dosage on DBP speciation in sewage under Fe(VI)-based process. (Page S15)
Fig S6. Effect of Fe(III) and Fe(VI) dosage on DBP speciation in sewage under Fe(VI)/ Fe(III)-based process. (Page S16)
Fig S7. Fluorescence EEM spectra of sewage after Fe(VI) coagulation. (Page S17)
Fig S8. Fluorescence EEM spectra of sewage after Fe(VI)/ Fe(III) coagulation. (Page S18)
Fig S9. Correlation heat map of different fluorescence indicators and DBP formation. (Page S19)

Text S1. Chemicals and reagents.

All solutions were prepared with analytical or higher-grade chemicals and purified water (18.2 MΩ cm). Potassium ferrate was purchase from Sinopharm Chemical Reagent Co. Ltd (Shanghai, China). Fe(VI) solutions were prepared prior to each experiment by diluting the desired amount (1.1-1.2 g) of solid $K_2Fe^{VI}O_4$ to DI water (10-15 mL). Fe(VI) solutions were filtered with 0.45 μm syringe filter membranes and used within 5 min. Caffeine (CAF) and paracetamol (PCT) stock solutions (10 mM) were prepared in ultra-pure water and ibuprofen (IBP) stock solutions (10 mM) were prepared in acetone. Ferric chloride ($FeCl_3$), Sodium thiosulfate ($Na_2S_2O_3$), sulfuric acid (H_2SO_4), sodium sulfate (Na_2SO_4), Sodium phosphate dibasic (Na_2HPO_4) and sodium phosphate monobasic (Na_2HPO_4), 2,2'-azino-bis(3-ethylbenzothiazoline-6-sulfonic) (ABTS) were purchased from Sinopharm Chemical Reagent Co. Ltd (Shanghai, China). High performance liquid chromatography (HPLC) grade methanol (MeOH), acetonitrile (ACN) were purchased from Boer Chemical Reagent Co., Ltd (Shanghai, China). The standards for trihalomethanes (THMs), haloacetaldehydes (HALs), haloacetonitriles (HANs) and halonitromethanes (HNMs) with the highest purity available were purchased from Sigma-Aldrich (St Louis, Missouri, USA), CanSyn ChemicalCorp. (Canada), and Aladdin Industrial Inc. (Shanghai, China). The detailed DBP information is available in Table S2.

Text S2. The measurement of fluorescence excitation-emission matrix (EEM).

EEM fluorescence spectra of the original sewage and treated samples were measured using a three-dimensional spectrofluorometer (F-7100 Fluorescence, HITACHI, Tokyo, Japan). Before the measurements, all of the samples were filtered with 0.45 μm syringe filter membranes and diluted tenfold (UV absorbance <0.05 cm^{-1} at 254 nm) to avoid inner-filtering effects (Yang and Hur, 2014). The fluorescence was scanned at a speed of 12000 nm/min in the wavelength range of (Ex, Em) = (200−450, 250−550 nm), with a slit width of 5 nm and a photomultiplier voltage of 400 V. Blank EEM spectra of ultrapure water was measured prior to sample analysis and used to subtract the water background. The obtained EEM data were then treated by eliminating first- and second-order Rayleigh and Raman scattering signals using an interpolation method and standardizing the unit of fluorescence intensity using the first-order Raman peak area of ultrapure water (Bahram et al., 2006; Lawaetz and Stedmon, 2009). The final fluorescent intensity was expressed in Raman Units (R.U.). Partition and fluorescence regional integration of five regions of EEM spectra were based on previous research and calculated using MATLAB R2019a (Chen et al., 2003).

Text S3. The measurement of size-exclusion chromatography-organic carbon detector (SEC-OCD).

The molecular weight distribution of DOM was measured by size-exclusion chromatography with an organic carbon detector (SEC-OCD). SEC was carried out using a polymethacrylate-packed column (250 mm × 20 mm, 3 μm), and installed on a Waters Alliance high performance liquid chromatography (HPLC, e2695, MA, USA) equipped with a Sievers M9 SEC organic carbon detector. Phosphate buffer (5.6 mM Na_2HPO_4/14.4 mM NaH_2PO_4) was used as the mobile phase and then was delivered with a HPLC pump at a flow rate of 1.0 mL/min to an autosampler (MLE,Dresden, Germany), and the injection volume was 250 μL. More information about SEC-OCD is available in a previous study (Zhang et al., 2021).

Text S4. UPLC conditions for emerging contaminants analysis.

PCT and IBP were detected with an HPLC (Agilent 1200) and equipped with an Waters C18 column (4.6 × 150 mm, 5.0 μm) with an injection volume of 100 μL, and a flow rate of 0.7 mL min^{-1} was used. Detection wavelengths for PCT and IBP were set at 273 and 220 nm, respectively. To eliminate interference from peaks of impurities from sewage and other oxidation products after treatment, a gradient elution was used to separate the intended peak. Both the mobile phases were methanol (A) and ultrapure water (B) for PCT. The gradient elution procedure for PCT was designed as follows: 0 min 30:70 (A%/B%), 3 min 30:70 (A%/B%), 7 min 70:30 (A%/B%), 9 min 30:70 (A%/B%), 13 min 30:70 (A%/B%). The mobile phases were acetonitrile (A) and 10mM phosphoric acid (B) for IBP. The gradient elution procedure for IBP was designed as: 0 min 20:80 (A%/B%), 9 min 90:10 (A%/B%), 10 min 20:80 (A%/B%), 13 min 30:70 (A%/B%).

Text S5. Quantification Method of Fe(VI).

The concentration of Fe(VI) stock solution was determined spectrophotometrically by measuring the absorbance at 510 nm using molar absorptivity ($\varepsilon_{pH\ 9}$ = 1150 M^{-1} cm^{-1}). The concentration of residual Fe(VI) at defined time intervals was determined by the ABTS method. ABTS solutions (450 μM) were prepared in 0.2 M phosphate/0.6 M acetate buffers at pH 4.0 and 4.0 mL of ABTS solutions was used for rapid reaction with 2ml of the sample at defined time intervals, to measure the absorbance at 645 nm ($\triangle A_{w/o}$) to calculated the concentration of residual Fe(VI) concentration. The concentration of Fe(VI) in sample was calculated by followed equation:

$$[Fe(VI)] = [ABTS^{\cdot +}]_{w/o} \div 1.02 \times 3 = \Delta A_{w/o} \div \varepsilon_{645} \div 1.02 \times 3$$

Where [Fe(VI)] represents the residual concentration of Fe(VI) in the samples collected at selected time intervals; $[ABTS\bullet+]_{w/o}$ represents the concentration of ABTS•+ produced from the reaction of Fe(VI) with ABTS; $\triangle A_{w/o}$ represents the change of the absorbance at 645 nm after completion of the reaction between Fe(VI) and ABTS.

Table S1. Major quality parameters for sewage.

DOC (mg/L)	NH_4^+−N (mg/L)	UV_{254}	Turbidity (NTU)	COD (mg/L)	TP (mg/L)
37	40	0.375	123	281	17.7

Table S2. Analytical methods and conditions for DBPs measurement.

GC/ECD:	QP2010plus, Shimadzu Corporation, Japan		
Columns:	RTX-5, 30 m × 0.25 mm ID, 0.25 μm film thickness		
Carrier gas:	Nitrogen, constant flow at 3 ml per minute.		
Injection volume:	1 μL		
Temperature programmes:			
Vaporizing chamber:	200 °C		
	for THMs	for HANs and HNMs	for HAMs
GC column	Initial temperature at 30 °C for 10.5 minutes, then 14 °C per minute to 72 °C and hold for 1 minute and finally 40 °C per minute to 200 °C and hold for 2 minutes.	Initial temperature at 30 °C for 10 minutes, then 17 °C per minute to 72 °C and hold for 1 minute and finally 40 °C per minute to 200 °C and hold for 2 minutes.	Initial temperature at 50 °C for 8 minutes, then 20 °C per minute to 120 °C and hold for 2 minutes and finally 40 °C per minute to 220 °C and hold for 5 minutes.
Detector:	300 °C		

Table S3. Characteristics, sources and limit of quantitation of the DBPs.

DBPs	CAS No.	Chemical formula	Molecular weight	LC_{50}（M）	Source and purity
TCM	67-66-3	$CHCl_3$	119.38	9.62×10^{-4}	Supelco, 99%
BDCM	75-27-4	$CHBrCl_2$	163.83	1.15×10^{-2}	Supelco, 99%
DBCM	124-48-1	$CHBr_2Cl$	208.28	5.36×10^{-3}	Supelco, 99%
TBM	75-25-2	$CHBr_3$	252.73	3.96×10^{-3}	Supelco, 99%
DCAL	79-02-7	$C_2H_2Cl_2O$	112.94	2.92×10^{-5}	Aladdin Industrial Inc.,99%
TCAL	75-87-6	C_2HCl_3O	147.39	1.16×10^{-3}	Aladdin Industrial Inc., 99%
DBCAL	64316-11-6	C_2HBr_2ClO	236.29	5.15×10^{-6}	CanSyn Chem Corp., 90~95%
TBAL	115-17-3	C_2HBr_3O	280.73	3.58×10^{-6}	Aladdin Industrial Inc., >90%
DCAN	3018-12-0	C_2HCl_2N	109.94	5.73×10^{-5}	Aladdin Industrial Inc., >90%
BCAN	83463-62-1	$C_2HBrClN$	154.39	8.46×10^{-6}	Accustandard, 99%
DBAN	3252-43-5	C_2HBr_2N	198.84	2.85×10^{-6}	Accustandard, 99%
MCNM	1794-84-9	CH_2ClNO_2	95.485	5.29×10^{-4}	Accustandard, 99%
DCNM	7119-89-3	$CHCl_2NO_2$	129.93	3.73×10^{-4}	CanSyn Chem Corp., >95%
BCNM	135531-25-8	$CHBrClNO_2$	174.38	4.05×10^{-5}	CanSyn Chem Corp., >95%
DBNM	598-91-4	$CHBr_2NO_2$	218.83	6.09×10^{-6}	CanSyn Chem Corp., >95%
TCNM	76-06-2	CCl_3NO_2	164.38	5.36×10^{-4}	State center for standard matter, 99%

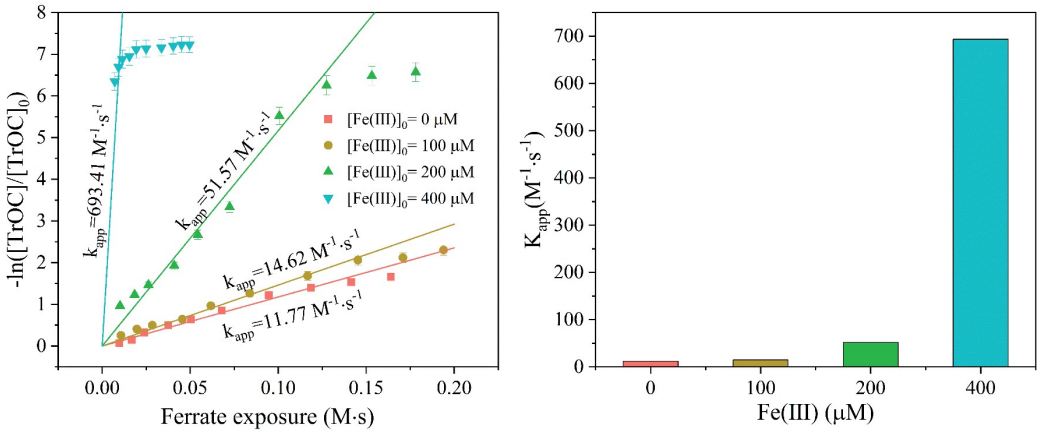

Fig S1. Fit of PCT oxidation by Fe(VI) with second-order reaction kinetics at different molar ratios of organics to Fe(VI). Experimental conditions: $[Fe(VI)]_0$ = 200 μM.

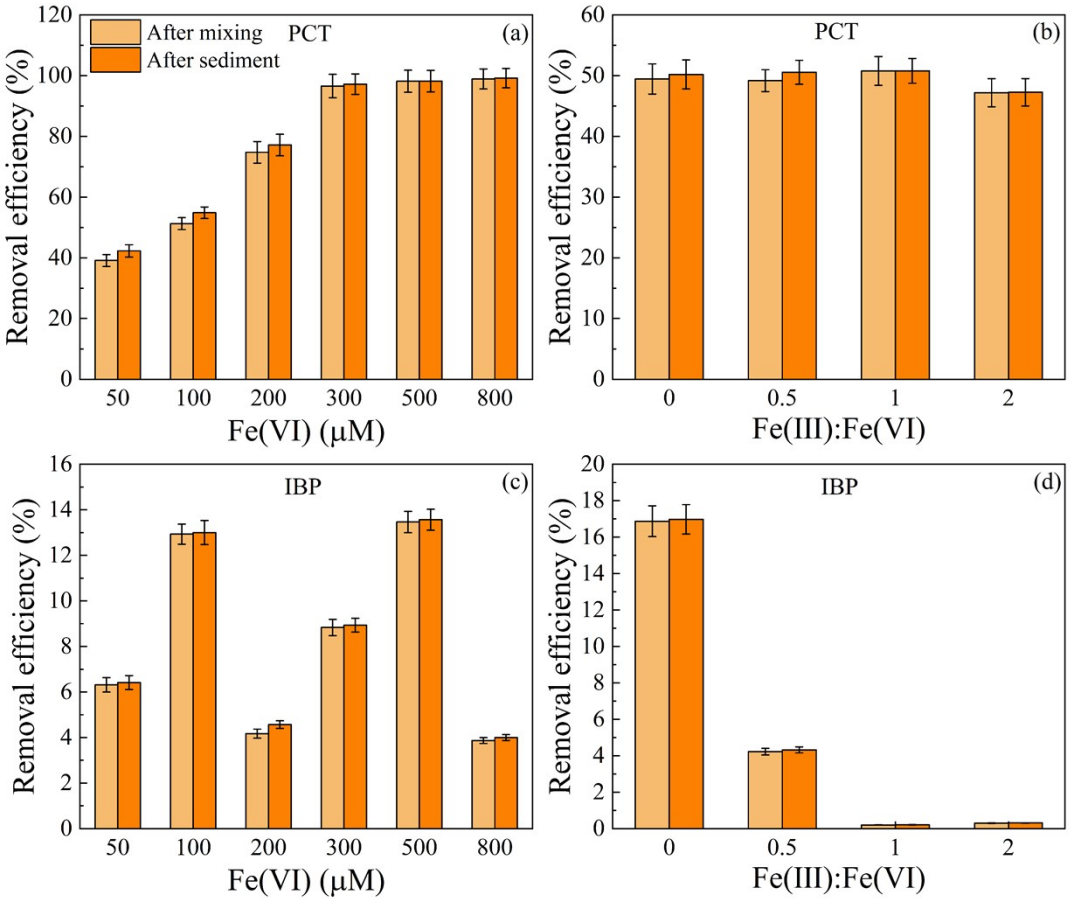

Fig S2. The actual removal of PCT (a, b) and IBP (c, d) by Fe(VI) and Fe(VI) /Fe(III) processes.

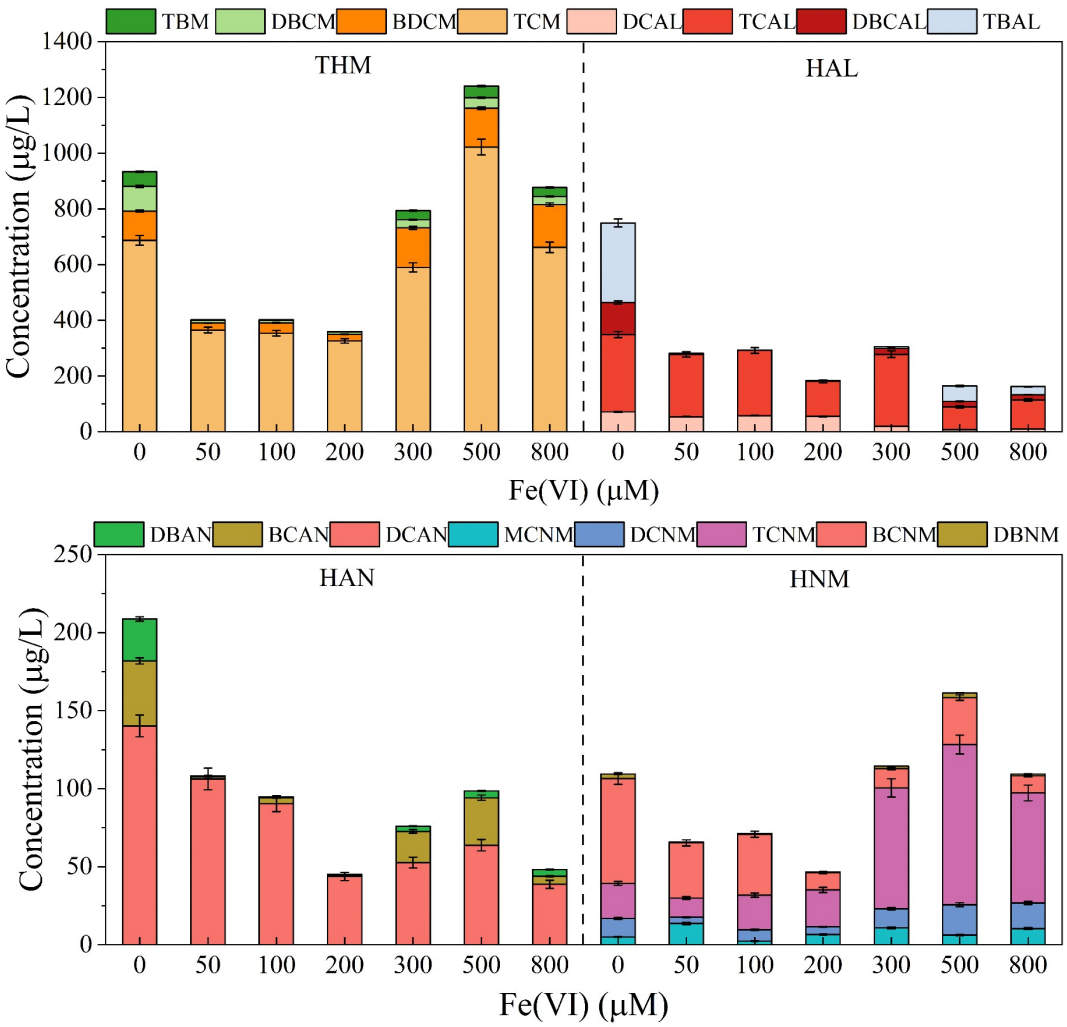

Fig S3. Effect of Fe(VI) dosage on DBP formation in sewage under Fe(VI)-based process.

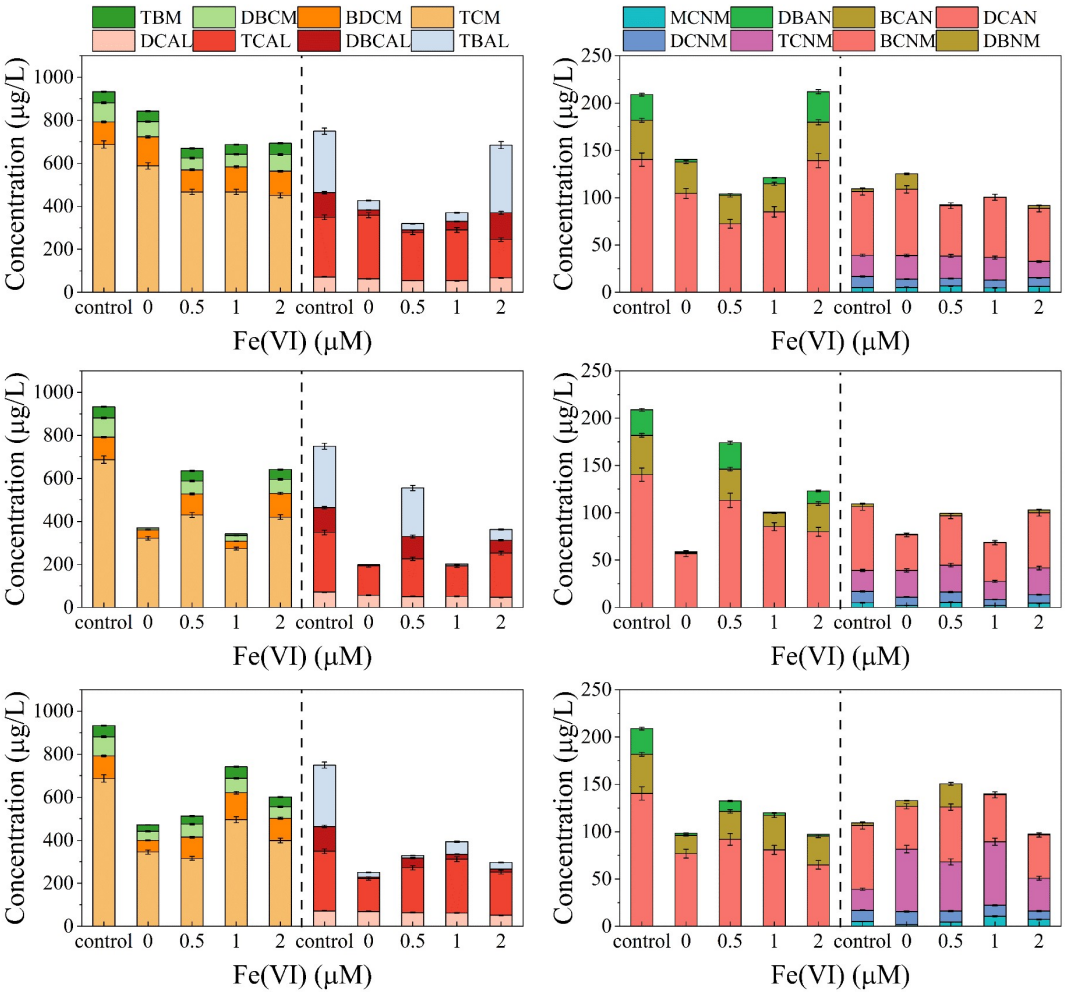

Fig S4. Effect of Fe(III) and Fe(VI) dosage on DBP formation in sewage under Fe(VI)/ Fe(III)-based process.

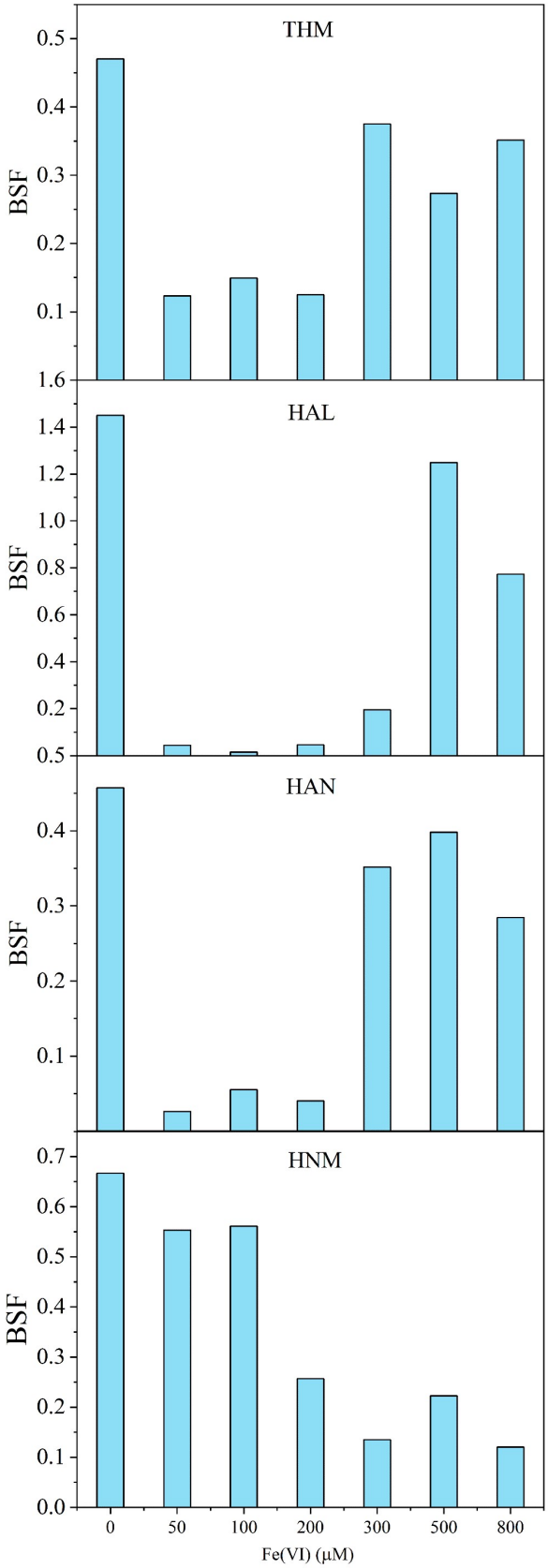

Fig S5. Effect of Fe(III) and Fe(VI) dosage on DBP speciation in sewage under Fe(VI)-based process.

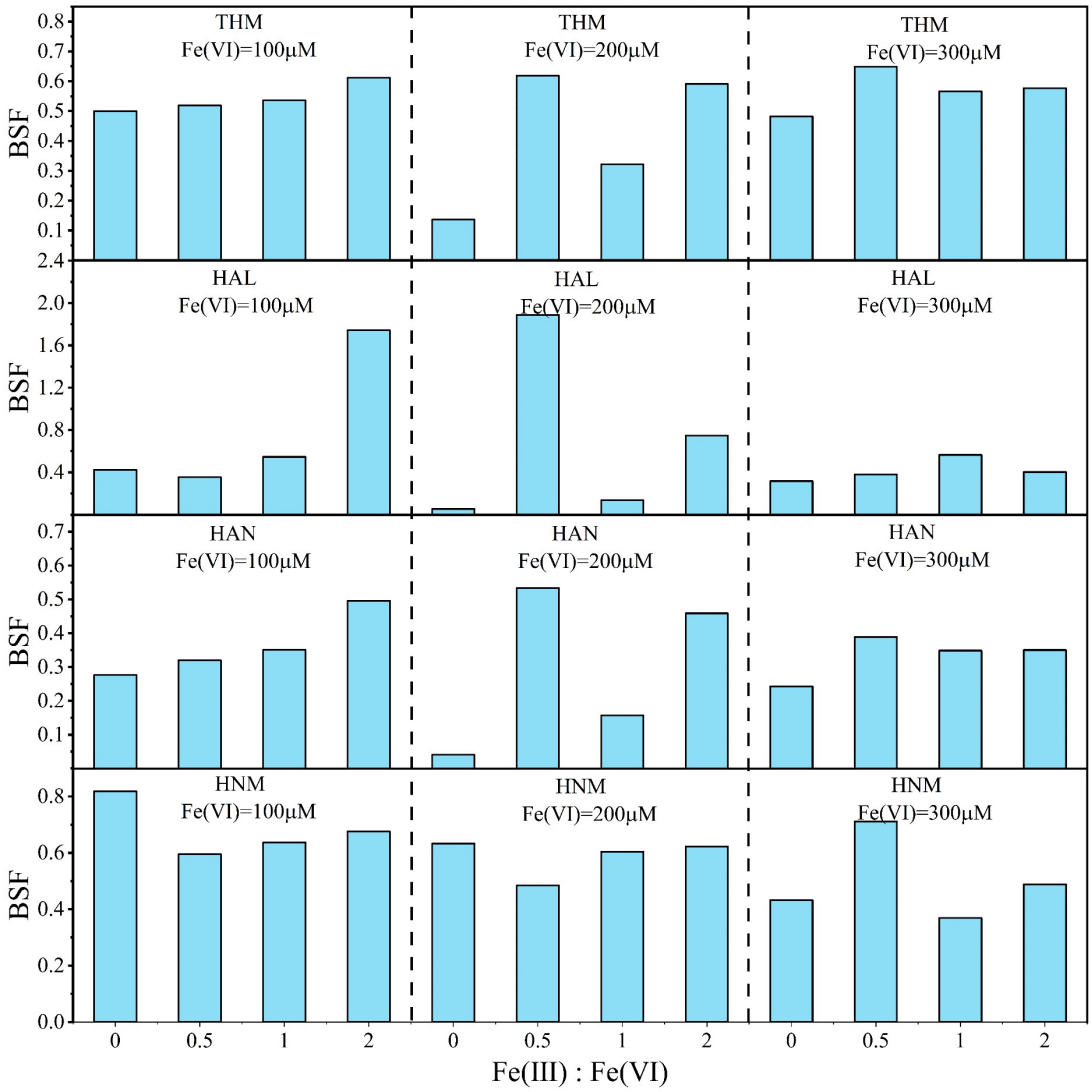

Fig S6. Effect of Fe(III) and Fe(VI) dosage on DBP speciation in sewage under Fe(VI)/ Fe(III)-based process

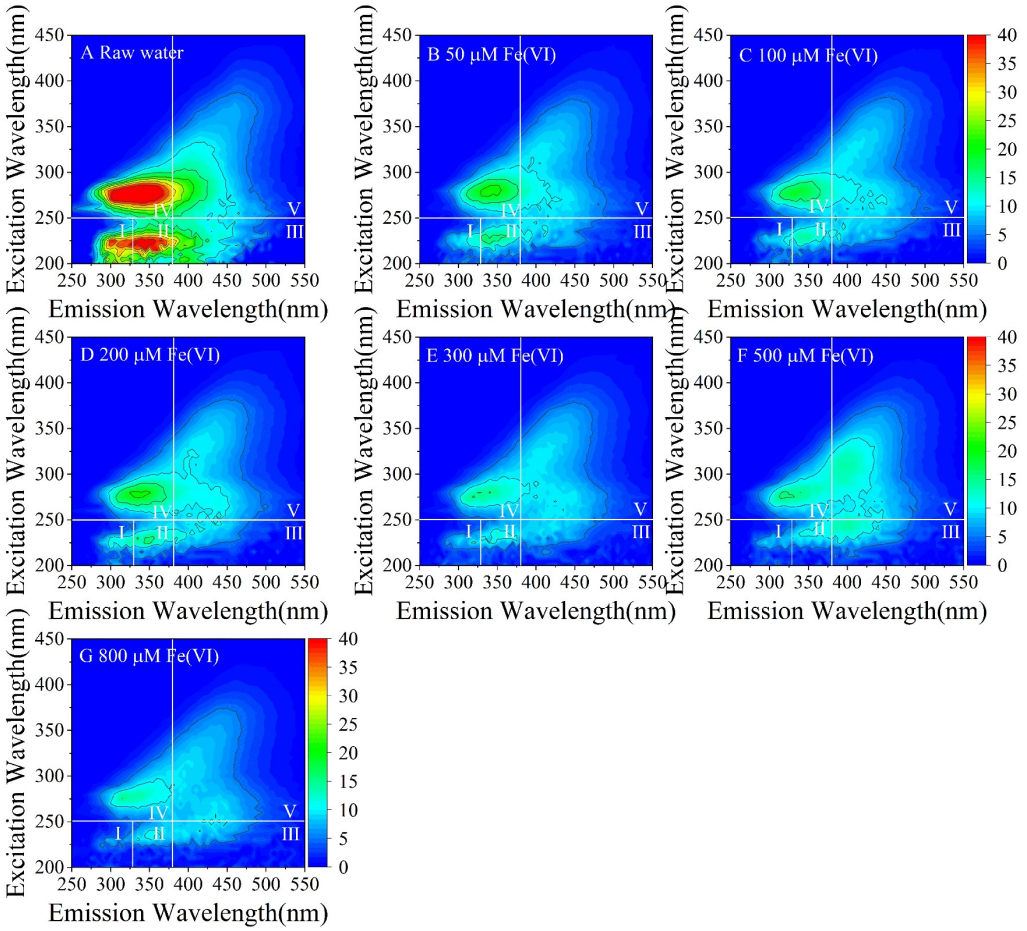

Fig S7. Fluorescence EEM spectra of sewage after Fe(VI) coagulation.

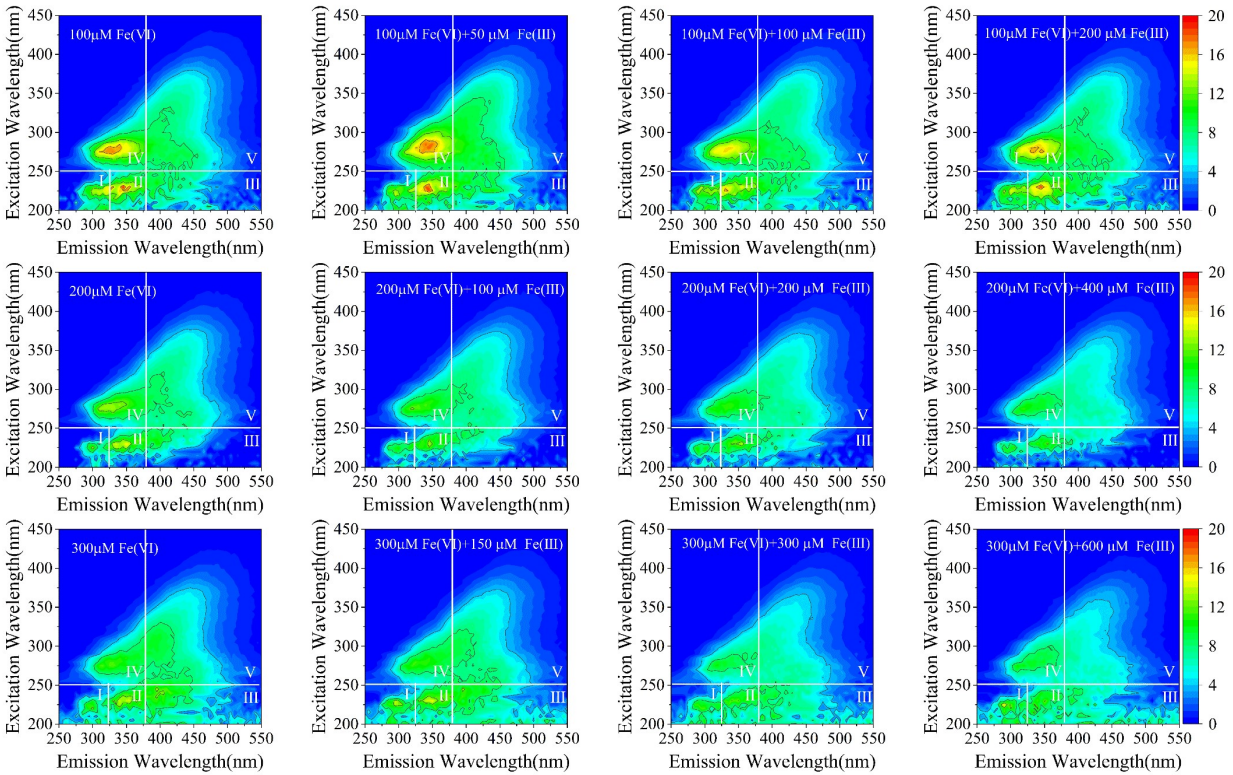

Fig S8. Fluorescence EEM spectra of sewage after Fe(VI)/ Fe(III) coagulation.

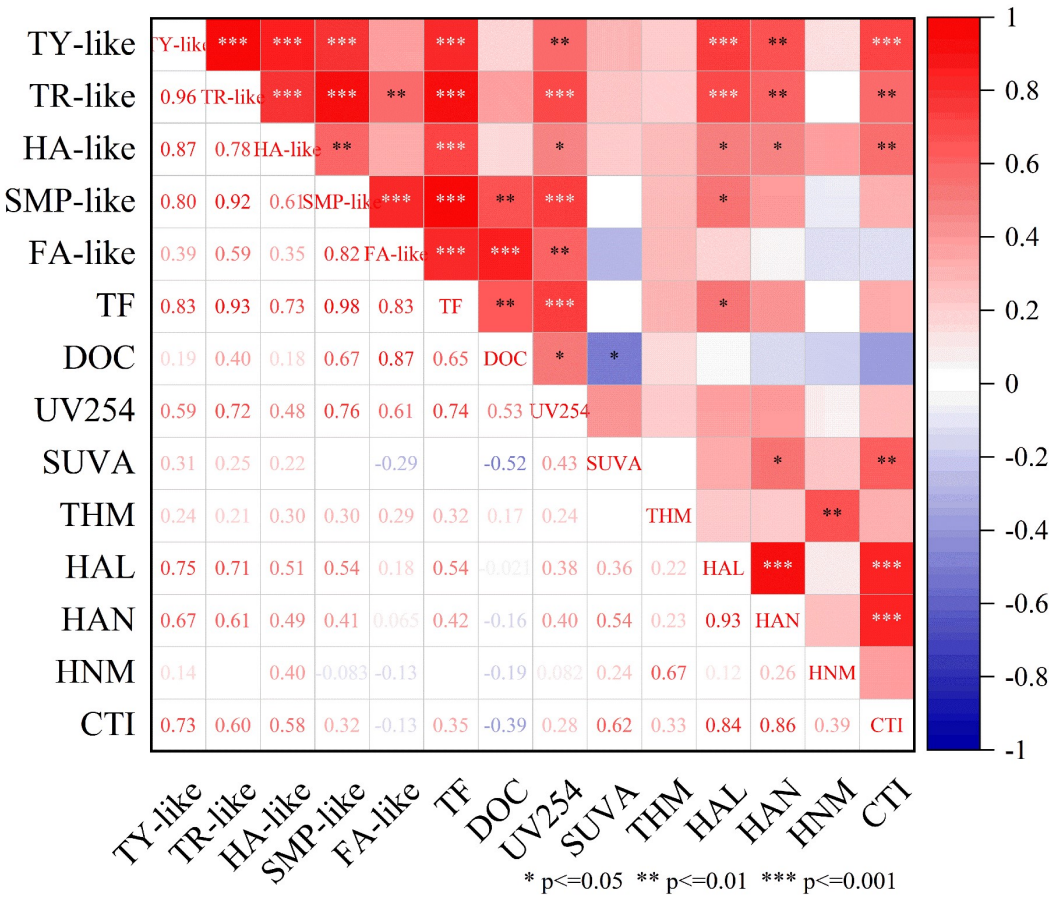

Fig S9. Correlation heat map of different fluorescence indicators and DBP formation.

Reference

Bahram, M., Bro, R., Stedmon, C. and Afkhami, A. 2006. Handling of Rayleigh and Raman scatter for PARAFAC modeling of fluorescence data using interpolation. JOURNAL OF CHEMOMETRICS 20(3-4), 99-105.

Chen, W., Westerhoff, P., Leenheer, J.A. and Booksh, K. 2003. Fluorescence excitation - Emission matrix regional integration to quantify spectra for dissolved organic matter. ENVIRONMENTAL SCIENCE & TECHNOLOGY 37(24), 5701-5710.

Lawaetz, A.J. and Stedmon, C.A. 2009. Fluorescence Intensity Calibration Using the Raman Scatter Peak of Water. APPLIED SPECTROSCOPY 63(8), 936-940.

Yang, L. and Hur, J. 2014. Critical evaluation of spectroscopic indices for organic matter source tracing via end member mixing analysis based on two contrasting sources. WATER RESEARCH 59, 80-89.

Zhang, D., Bond, T., Li, M.L., Dong, S.K., Pan, Y., Du, E.D., Xiao, R. and Chu, W.H. 2021. Ozonation Treatment Increases Chlorophenylacetonitrile Formation in Downstream Chlorination or Chloramination. ENVIRONMENTAL SCIENCE & TECHNOLOGY 55(6), 3747-3755.